Sensitivity of screen printed WO_3 thick film chemiresistance gas sensor with alteration in firing temperature

Kaveri B. Bhamare

Mahatma Gandhi Vidyamandir's L. V. H. Arts, Science and Commerce College,
Panchavati, Nashik-03, Maharashtra, India.

***Abstract*: The main aim of the study was to find the effect of firing temperature on the nature of tungsten trioxide thick film prepared by screen printing process for gas sensing application. X-Ray diffraction is used to examine the phases formed after firing. XRD result shows a mixture of monoclinic, orthorhombic phases of WO_3 in the range 600°C-800°C. The morphology was analyzed by SEM-EDS. The D.C. resistance of the films was measured by half bridge method in air atmosphere in 30°C to 450°C temperature range. The WO_3 films showed semiconducting nature. The temperature coefficients of resistance, activation energy, sheet resistivity and surface area to volume ratio of films were assessed at different firing temperatures. Surface area to volume ratio decides the gas sensing property of the film. The cause of the enhancement of gas sensitivity of the sample for target gas with high surface area to volume ratio was also discussed. Gas sensing property ameliorates for greater ratio. Film fired at 600°C has maximum ratio hence found to be suitable for gas sensing.**

***Keywords*: WO_3, screen printing, SEM, XRD, resistivity.**

I. INTRODUCTION

Air, a nature's gift and a valuable asset is one of the most important elements of environment which is freely available for our survival. Unfortunately, due to industrialization it is far from pure at the moment. Ironically, although industrialization has improved human lives on one hand; on the other hand it is adversely affecting the human health due to pollutants from industrial emissions, exhaust gases from the vehicles and aircrafts etc. Land vehicles use oil and fuel which create smoke which gets mixed with air and thus pollutes air. A number of physical activities (volcanoes, fire, etc.) may liberate different pollutants in the nearby area; anthropogenic activities are the major cause of environmental air pollution.

Thus, there is a need of gas sensors to measure the pollution level in the atmosphere so that the appropriate steps can be followed to control the pollution. In addition, to protect against the unwanted incidence of fire or explosion, the flammable gases need to be regulate for useful purpose. Thus development of reliable, low cost, low power gas sensors with better sensitivity and selectivity towards specific gases is growing demand of research.

The development of MOS gas sensors started from the work of Brattain and Bardeen in the late 1940s [**1-3**] who clarified that the resistance of semiconductors was very sensitive to adsorption of gas molecules present nearby the sensing element. They described the effect of the ambient atmosphere upon the electrical conductance. Just after the discovery of sensing process Seiyama et al. in 1962 practically proved the effect of ambient gases on conductivity of ZnO films. The sensitivity was found to be maximum at 300°C [**4**]. In 1970 Taguchi demonstrated that SnO_2 was sensitive to the reactive gases in the atmosphere [**5-7**]. Since then, for gas-leak indicator, process control, pollution control, etc. semiconductor gas sensors have been extensively used as domestic and industrial gas detectors Compared to the organic (such as phenenthrene, polybenzimidole) and elemental (such as Si, Ge, GaAs, GaP) semiconductors, semiconductor oxides have been more successfully employed as sensing materials for the detection of different gases, such as CO, CO_2, H_2, alcohol, NH_3, O_2, NO_x, etc. Both p-type and n-type semiconductor oxides can be used as gas sensor materials. For the development and study of solid state gas sensor, vast amount of literature was developed.

Various semi conducting metal oxides SnO_2 [**8-9**], ZnO [**10-11**], WO_3 [**12, 13**], In_2O_3 [**14**]; catalytic oxides V_2O_5 [**15**], MoO_3 [**16**], CuO [**17**], NiO [**18**] and mixed oxides lanthanum ferrite: $LaFeO_3$[**19**], zinc ferrite: $ZnFe_2O_4$ [**20**], Barium titanate: $BaTiO_3$ [**21**] and $Cd_2Sb_2O_{6.8}$ [**22**] have been studied for gas detection and many more new oxides are currently being explored.

For the detection of toxic, pollutant gases, combustible gases and organic vapours metal oxide semiconductors have been used enormously. It is reported that tungsten oxide (WO_3) films have promising optical & electrical properties. WO_3 is an n-type semiconductor. The band gap of WO_3 is about 2.6 -2.8 eV [**23**]. WO_3 has perovskite-type ABO_3 lattice in which 'A' site remains unoccupied. The WO_3 is considered as oxygen-deficient or nonstoichiometric oxide has many oxidation states i. e. 2, 3, 4, 5 and 6. C. V. Raman proved the phase transformations in the WO_3 films by annealing in the TEM column at 30°C to 500°C [**24**]. The crystal structure of tungsten trioxide is temperature dependent, shows five phase transitions in accordance to the following sequence: triclinic from – 50°C to 17°C, monoclinic from 17°C to 330°C, orthorhombic from 330 to 740°C and It is tetragonal above 740°C. An intermediate meta-stable form of WO_3 is hexagonal tungsten trioxide. Such electronic properties make the tungsten oxides suitable for gas sensors [**25**].

The working principle involves the receptor function controlled by the surface of each oxide grain and the transducer function controlled by each grain boundary. The third factor, utility, determines the effective utilization of surface and bulk grains for the ambient gas response [**26**].

The aim of present work is to prepare WO_3 thick films by screen printing technique on alumina substrate and to explore its characteristics after treating with different firing temperature.

II. EXPERIMENTAL WORK

The WO_3 powder (Sigma Aldrich, AR grade, purity 99.99 %) was weighed accurately by contech high precision digital balance. and calcined for 2 hours at 450°C. The calcined WO_3 powder was mixed thoroughly with ethyl cellulose as a temporary binder and glass frit as permanent binder. The mixture was then mixed with right proportion of butyl carbitol acetate (BCA) to make the paste of suitable viscosity. The proportion of binder and vehicle to make paste is tabulated in Table 1:

Table 1: Composition of material

Material		Proportion (gm)
Inorganic (70 %)	WO_3	95 % of 70%
	Glass frit	5 % of 70%
Organic (30 %)	BCA	92 % of 30%
	EC	8 % of 30%
∗For x % additives, WO_3 will be (95- x) %		

The paste was used to prepare thick films on alumina substrate by using standard screen printing technique [**27, 28**]. After the printing, films so produced were exposed at room temperature for 2 to 3 hours so as to settle down the paste in the form of film. The films were dried under IR-lamp for nearly 1 hour to remove the temporary organic binder. The films were fired at 600°C, 700°C and 800°C separately for nearly 3 hour to obtain stability and better adhesion of the film on the alumina substrate. The thicknesses of the films were measured and found to be in the range from 10 μm to 25 μm by gravimetric weight-loss method.

The DC resistance of the films at different temperature was measured by using half bridge method. The films were set in a temperature controlled atmosphere to maintain the fixed temperature. To record the operating temperature digital temperature controller system with chromelalumel thermocouple was used. The grain size, resistivity, activation energy and TCR were evaluated from the observed data in the temperature range 30°C to 450°C.

III. RESULTS AND DISCUSSION:

Structural analysis:

The XRD patterns are obtained with Rigaku, D. Max 2200 diffractometer operating at tube current and voltage 40 mA and 40mV, respectively using monochromatic Cu-Kα radiation. Diffraction patterns were registered on the photographic film by scanning at 2θ from 10° to 80° at a rate of 15 deg /min. The observed peaks in figure (1) are perfectly matched very well with ICDD card no. 20-1324 and 43-1035 indicating presence of monoclinic and some orthorhombic phases of WO_3. The intensity and sharpness of the peaks goes on increasing with the increase of firing temperature indicating crystallinity of WO_3 thick films. The crystalline size (D) was estimated for the sharp intense peak at the hkl plane [200] by Debye–Scherer's formula. The calculated values for crystalline size are tabulated in Table 2.

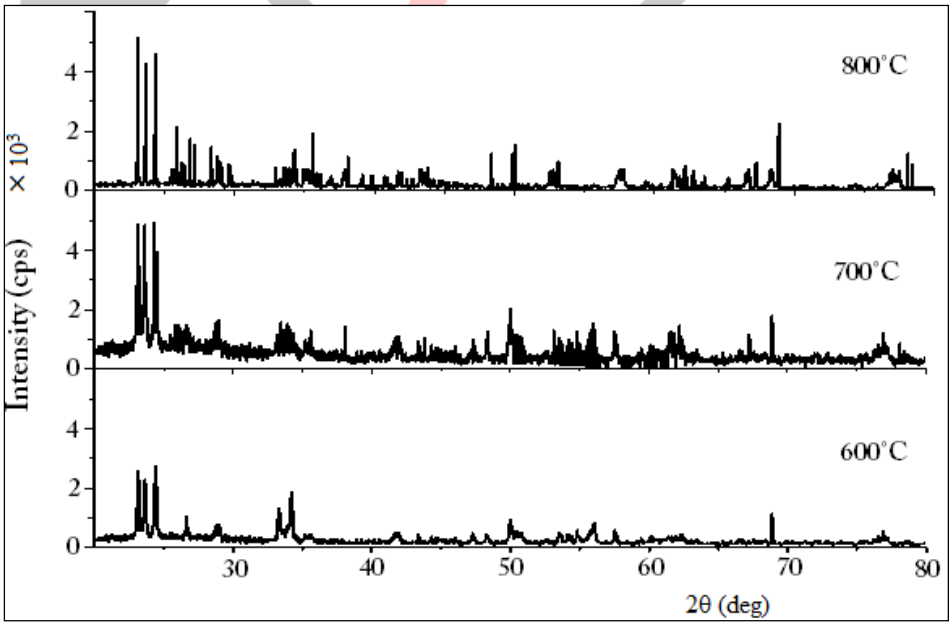

Figure 1: XRD diffractogram of WO_3 thick film fired at (a) 600°C (b) 700°C and (c) 800ºC

Surface Morphology Analysis:

The morphology was observed by scanning electron microscopy (JEOL JSM 6360 model). Figure (3) shows SEM images of WO_3 films fired at different firing temperatures.

It clearly showed that the surface of WO_3 film is porous and forms channels with bundles of grains. Therefore, the screen printed WO_3 film can adsorb atmospheric oxygen due to large exposed surface area of the film. J. D. Mackenzie et al. showed that highly porous film sensors have high sensitivity for gas detection and their finding proved very well [**29**]. The gas sensing film gets modulated when exposed to gas under study as shown in figure (2).

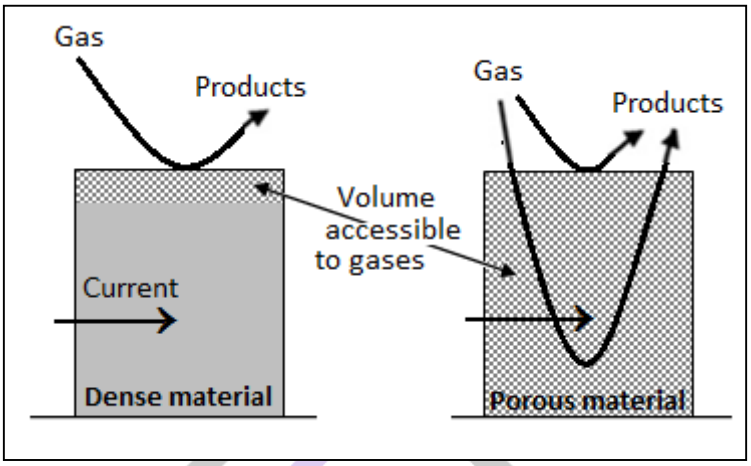

Figure 2: Material density influence on gas penetrability

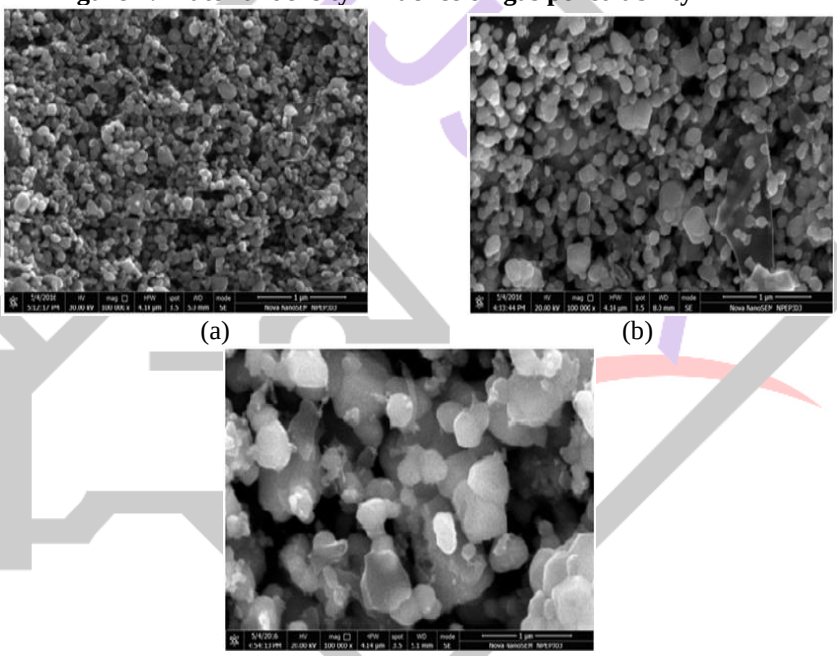

Figure 3: SEM microphotograph of WO_3 film at firing temperatures (a) 600°C (b) 700°C (c) 800°C

Table 2: Different parameters estimated from XRD, SEM and EDAX of WO_3 thick films.

Firing Temperature (°C)	Crystallite size (± 2 nm) (nm)		Specific surface area (m^2/g)
	XRD	SEM	
600	52.03	93.35	8.98
700	55.86	174.19	4.81
800	59.90	273.8	3.06

Table 3: Element composition

Firing temperature	Element	At. Wt. %	W/O ratio	Mass %	W/O ratio

600 °C	W	66.19	1.9577	95.74	22.474
	O	33.81		4.26	
700 °C	W	69.47	2.2754	96.32	26.174
	O	30.53		3.68	
800 °C	W	72.12	2.5868	96.74	29.675
	O	27.88		3.26	

It is clear from Table 3 that the weight percentage of tungsten is increased with firing temperature. The thick film fired at 600°C observed to be large specific surface area which make possible to adsorb a large amount of oxygen species which increases the gas sensitivity [**30, 31**]. Therefore films fired at 600°C were used for gas sensing application for further work.

Electrical characteristics:

Negatively charged oxygen adsorbates play an important role in detecting inflammable gases. Actually several kinds of oxygen adsorbates such as O_2^-, O^-, and O^{2-} are known to cover the surface of semiconductive metal oxides in air [**32**]. Of these O minus is the most reactive with inflammable gases in the temperature range of 300-500 °C, in which most semiconductor gas sensors are operated, and eventually the variation in surface coverage of O^- changes the sensor resistance.

For n- type material, the formation of these oxygen adsorbates builds a space-charge region on the surfaces of the metal-oxide grains, resulting in an electron depleted surface layer due to electron transfer from the grain surfaces to the adsorbates as follows [**33**]:

$$\tfrac{1}{2}O_2(gas)+2e^- = 2O^-(ad) \quad (1)$$

The resulting equations are,

$$O_2\ (gas) \rightleftarrows O_2\ (ads) \quad (2)$$

$$O_2\ (ads) + e^-\ (bulk) \rightleftarrows O_2^-\ (ads) \quad \text{at } 100 - 150°C \quad (3)$$

$$O_2\ (ads) + 2e^-\ (bulk) \rightleftarrows 2O^-\ (ads) \quad \text{at } 150 - 300\ °C \quad (4)$$

$$O^-\ (ads) + e^-\ (bulk) \rightleftarrows O^{2-}\ (ads) \quad \text{at } 300- 500°C \quad (5)$$

$$V_{0^{\cdot\cdot}} + 2e^- + 1/2\ O_2 \rightleftarrows O_{lattice} \quad (6)$$

Intrinsic electron concentration in the bulk and surface coverage of oxygen adsorbates decides the depth of this space-charge layer (L). The resistance of an n-type semiconductor gas sensor in air is therefore high, due to the development of a potential barrier to electronic conduction at each grain boundary as shown in figure 4 [**34**]. When the sensor is exposed to target gas at elevated temperatures, the oxygen adsorbates are cancelled by the subsequent reactions and lower steady-state surface coverage of the adsorbent is developed. During this process the electrons trapped by the oxygen adsorbates return to the oxide grains of the sensor film, leading to a decrease in the potential barrier height and a drop in resistance. This resistance change is used as the measurement parameter of a semiconductor gas sensor, with sensitivity defined as:

$$\text{Sensitivity} = \left|\frac{R_{air} - R_{gas}}{R_{air}}\right| = \frac{\Delta R}{R_{air}} \quad (7)$$

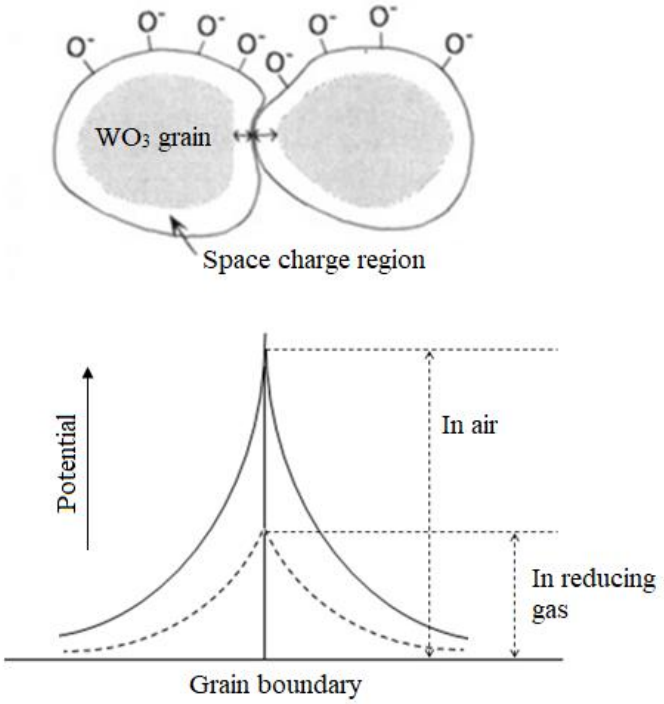

Figure 4: A model of a potential barrier to electronic conduction at a grain boundary.

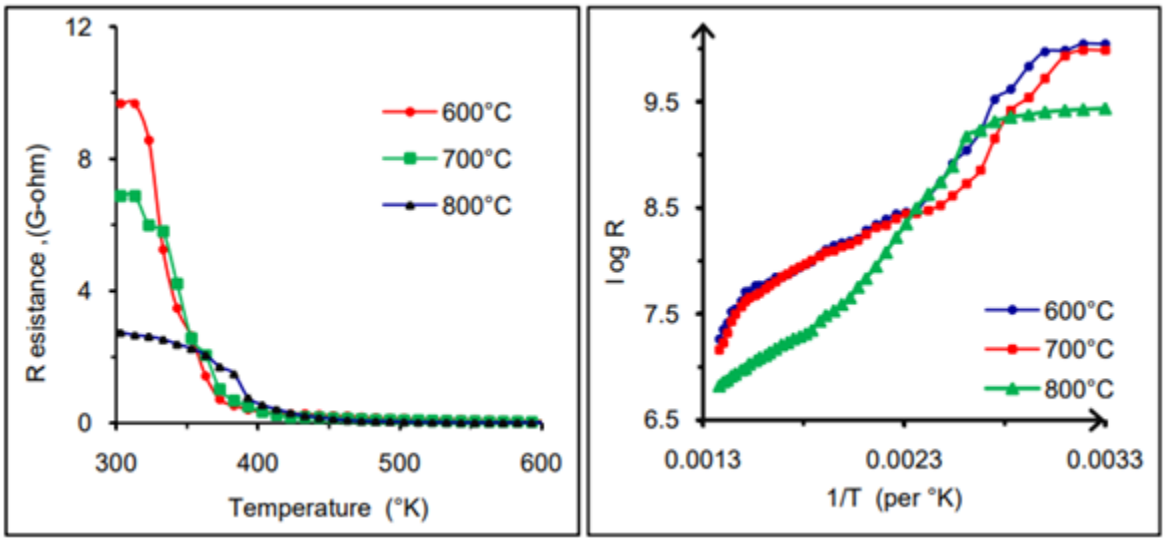

(a) (b)

Figure 5: Variation of (a) R Vs T (b) log R Vs $\frac{1}{T}$ of WO_3 thick films fired at 600°C, 700°C, 800^{0}C.

The transition temperatures for the films fired at 600 °C, 700 °C and 800 °C are 160, 140 and 110 °C respectively.

The initially value of WO_3 thick film resistance in air atmosphere at 30 °C was 9667, 6882, 2742 MΩ fired at 600, 700, 800°C respectively may be due to change in thickness of the film.

To determine the activation energy, the variation of electrical resistance as a function of inverse of temperature in the temperature range of 323°K to 568°K is studied and shown in figure 5(b). It is observed that electrical resistance decreases with increase in temperature as shown in figure 5(a). The activation energy in the low temperature region is always less than the energy in the high temperature region because material passes from one conduction mechanism to another [35].The variation of resistivity, temperature coefficient of resistance (TCR) and activation energy of the WO_3 thick films summarized in Table 4.

Table 4: Electrical parameters of WO_3 Film samples fired at different temperature (t=16 µm).

Firing temp.	Film	Thickness (µm)	ρ at room temp (Ωm)	ρ_s ,Sheet resistivity (□/Ω) $\times 10^{10}$	TCR at 100°C (ppm /°K)	Activation energy ΔE (eV)	
						LTR	HTR
600°C	F1	12.48	102748	0.823	908.37	0.3356	0.4447
	F3	13	102727	0.790	907.80	0.3356	0.4449
	F5	16	103119	0.644	903.26	0.3350	0.4449
700°C	F1	12.51	73774	0.591	2456	0.3555	0.3878
	F3	13.02	73095	0.562	2396	0.3541	0.3934
	F5	16.04	73412	0.459	2468	0.3551	0.3950
800°C	F1	12.54	29282	0.235	10083	0.2159	0.2483
	F3	13	26444	0.203	9904	0.2154	0.2485
	F5	15.92	29251	0.183	10124	0.2157	0.2484

It is observed that the resistivity, activation energy decreases where as TCR and grain size increases with increasing firing temperature. These results may be assigned to increase in the degree of crystallinity with the firing temperature. Apart from this phenomenon Tadasi T. also observed drop in semiconductor resistance with rise in temperature as exothermic reaction of the gases takes place with the surface oxygen adsorbates [**36**].

Gas sensing response film fired at 600°C:

Figure 6 shows the pure WO_3 thick film gas sensor response for LPG, C_2H_5OH, H_2S, NH_3, O_2 and NO_2 to 500 ppm. WO_3 Gas sensing response was measured in air at a temperature range 100° to 450°C. The temperature scan rate used for the study gas sensing response is nearly constant and slow (≈10°C/min). Sensors were not sensitive to test gas at room temperature. The higher temperature enhances surface reaction of the sensor and gives higher sensitivity for ambient gases. Amount of chemisorbed oxygen on surface and the surface species available for adsorption highly influences the change in conductivity. The pure WO_3 thick films show considerable response to NO_2 gas. The resistance of films increases when exposed to the NO_2 gas. The maximum sensitivity observed for NO_2 is 24.31 at 290 °C which is higher than other studied gases [**37**].

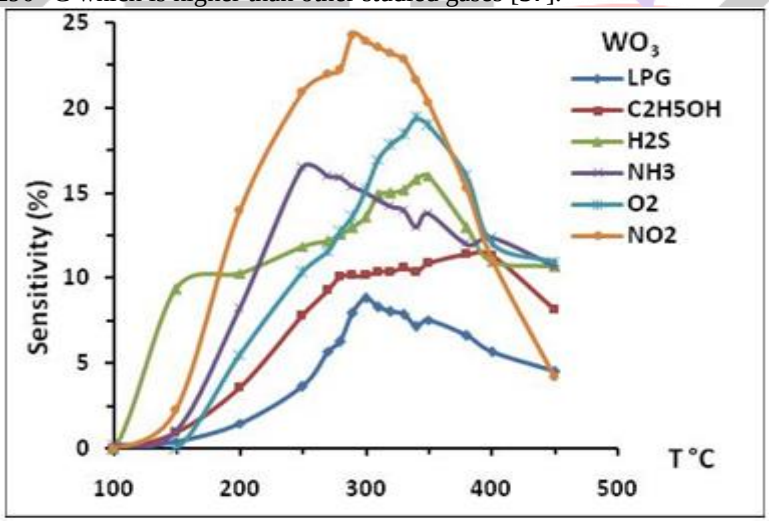

Figure 8: Plot of sensitivity Vs temperature of WO_3 thick films for different gases

CONCLUSIONS

This work demonstrated the successful preparation of WO_3 screen printed thick film. These thick films were characterized by using XRD and SEM coupled with EDAX. The XRD pattern reveals that the screen-printed thick films were polycrystalline in nature. The thick films were used to study influence of firing temperature on the gas sensing properties of film. It is observed that crystallinity of the film increase with increase in firing temperature but beyond specific limit affect the morphology of the film. Film fired at 600°C shows maximum sensitivity is 24.31 at 290 °C for NO_2 with fast response (~ 16 s) and recovery time (~ 42 s).

With drop in firing temperature, crystallite size decreases but specific surface area increases which is necessary condition for gas sensing phenomenon as more ambient oxygen molecules get adsorbed on the sensor film. The average particle size observed in SEM is much higher than estimated from bulk XRD data, indicating agglomeration of the particles. The film fired at 600°C has

better adhesion to alumina surface, offer high resistivity, low TCR and grain size. The average grain size of the WO_3 was found to be nearly 52.03 nm which is slightly less than the earlier reported values.

REFERENCES:

[1] P. T. Moseley, Sens. Actuators B 3 (1991) 167-174.
[2] P. K. Clifford and D. T. Tuma, Sens. Actuators B Chem. 3 (1982-83) 233-281.
[3] N. Barsan, D. Koziej and U. Weimar, Sens. Actuators B Chem. 121 (2007) 18-35.
[4] T. Seiyama, A. Kato, K. Fujiishi, M. Nagatani, Anal. Chem. 34 (1962) 1502-1503.
[5] N. Taguchi, Japan Pat. 45-38200 (1962).
[6] N. Taguchi: Japanese Patent 45-38200.
[7] N. Taguchi: Japanese Patent 47-38840. 4 N. Taguchi: US Patent 3 644 795.
[8] A. S. Garde, Research Journal of Recent Sciences 4 (1) (2015) 55-61.
[9] B. Panchapakesan, D. L. Devoe, M. R. Widmaer, R. Cavicchi et al. Nanotechnology 12 (2001) 336-349.
[10] A. V. Patil, C. G. Dighavkar, R. Y. Borse, Sensors & Transducers Journal 101(2)(2009) 96-103.
[11] S. D. Shinde, G. E. Patil, D. D. Kajale, V. G. Wagh et al, International Journal on Smart Sensing and Intelligent System 5 (1) (2012) 277-294.
[12] R. S. Khandayte, J. V. Sali, P. P. Patil, Sensors & Transducers J. 76 (2) (2007) 1001-1007.
[13] L. G. Teoh, I. M. Hung, J. Shieh, W. H. Lai et al. Electrochemical and Solid-State Letters 6 -8 (2003) G108.
[14] D. N. Chavan, G. E. Patil, D. D. Kajale et al. , Sensors and Transducers Journal, 125 (2) (2011) 142-155.
[15] Wei Jin, Wen Chen, Bai Tao Dong, et. al , Key Engineering Materials 421 (2009) 328.
[16] A. A. Firooz, A. R. Mahjoub, A. A. Khodadadi, J. Nanosci Nanotechnol. 10(9) (2010) 6155-6160.
[17] P. Samarasekara, N. T. R. N. Kumara and N. U. S. Yapa, J. Phy.: Condens. Matter 18 (2006) 2417.
[18] M. Stamataki, D. Tsamakis, N. Brilis, I. Fasaki et al., Physica Status Solidi A-Applied Research 205 (2008) 2064–2068.
[19] H. T. Fan, X. J. Xu, X. K. Ma, T. Zhang, Nanotechnology 22 (11) (2011) 115502.
[20] Chu Xiangfeng, Liu Xiangqin, M Guangyao, Sens. Actuators B 55(1) (1999) 19.
[21] G. H. Jain, L. A. Patil, P. P. Patil et. al , Bulletin of Material Science 30 (2007) 9.
[22] F. Gao, Y. Liu and X. Liu, Sens. Actuators B Chem. 77 (3) (2001) 653-656.
[23] L. Ottaviano, F. Bussolotti, L. Lozzi , M. Passacantando, Thin Solid Films 436 (1) (2003) 9-16.
[24] C. V. Ramana, S. Utsunomiya, R. C. Ewing et. al, J. Phys. Chem. B 110 (21) (2006) 10430–10435.
[25] B. Krishnanv, P. N. Nampoori, Bulletin of Materials Science, Thin Films 28 (3) (2005) 239-242.
[26] N. Yamazoe, Sensors and Actuators B 108 (1-2) (2005) 2–14.
[27] Maria Prudenziati, Thick Film Sensors, Volume 1, 1st Ed. Handbook of Sensors and Actuators, Elsevier Science, 26th August 1994.
[28] N. M. White and J. D. Turner, "Thick-film sensors: past, present and future," Measurement Science and Technology 8 (1) 1997.
[29] Sung-Soon Park, J. D. Mackenzie, Thin Solid Films 274 (1-2) (1996) 154-159.
[30] Jiaqiang Xu, Qingyi Pan, Yu'an Shun, Zhizhuang Tian, Sensors and Actuators B: Chemical 66 (1-3) (2000) 277-279.
[31] K. Arshak, I. Gaidan , Materials Science and Engineering: B 118 (1-3) (2005) 44-49.
[32] Barsan, N.; Weimar, U. Conduction model of metal oxide gas sensors. J. Electroceram. 2001, 7, 143-167.
[33] Yasuhiro Shimizu and Makoto Egashira , Basic Aspects and Challenges of Semiconductor Gas Sensors, Material Research Society Bulletin, MRS Bulletin , 24(6) (1999)18 – 24.
[34] Oehme, F., "Liquid Electrolyte Sensors; Potentiometry, Amperometry and Conductivity" in Sensors, edited by Gopel, W., Hesse, J., and Zemel, J.N. (VCH, 1991).
[35] I. S. Ahmed Frag, I. K. Battisha, M. M. EI_Rafaay, Indian J. Pure Appl. Phys. 43 (2005) 446.
[36] TadashiTakada, Temperature drop of semiconductor gas sensor when exposed to reducing gases — simultaneous measurement of changes in sensor temperature and in resistance, Sensors and Actuators B: Chemical 66(1-3) (2000) 1-3.
[37] K. B. Bhamare, T. R. Mahale, R. Y. Borse "Preparation and Characterization of Tungsten Oxide Thick Film Gas Sensor" International Journal of Engineering Science Invention (IJESI) 7(7) (2018) 66-77.